eLIFE elifesciences.org

RESEARCH ARTICLE

Figures and figure supplements

A SLC4 family bicarbonate transporter is critical for intracellular pH regulation and biomineralization in sea urchin embryos

Marian Y Hu *et al*

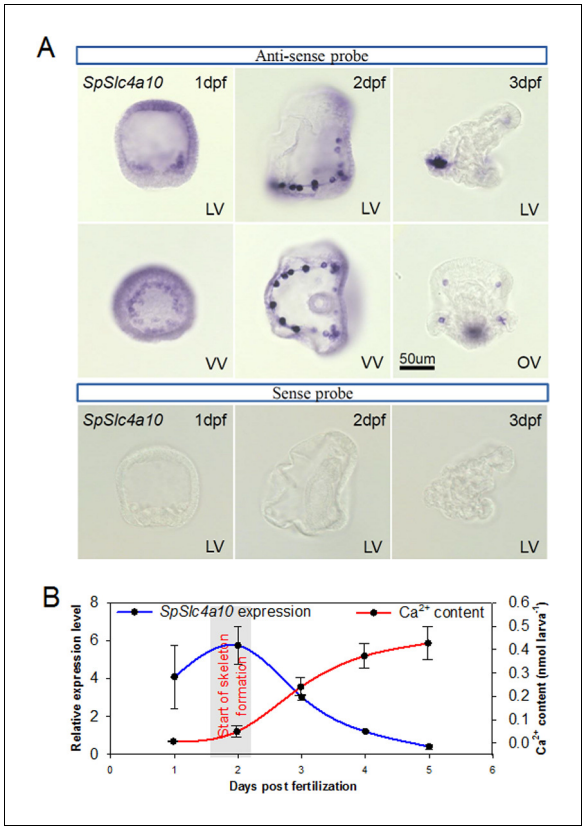

Figure 1. Expression pattern of the *SpSlc4a10* gene from blastula through pluteus larva in *Strongylocentrotus purpuratus*. (**A**) Localization of *SpSlc4a10* expression in the sea urchin larva along the larval development until 3 days post fertilization (dpf). Expression was detected in primary mesenchyme cells (PMCs) of the late blastula stage forming a ring around the blastopore. In the early pluteus larva *SpSlc4a10* expression is exclusively found in PMCs located at ends of the spicules. (**B**) *SpSlc4a10* expression levels and total calcium content along the early development of sea urchin larvae raised under control conditions. Bars represent mean ± SD; *n* = 3. dpf: days post fertilization; LV, lateral view; VV, vegetal view; OV, oral view.
DOI: https://doi.org/10.7554/eLife.36600.003

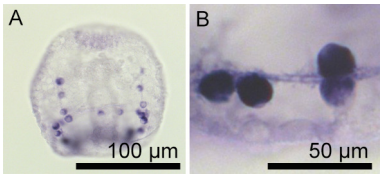

Figure 1—figure supplement 1. Expression of *SpSlc4a10* in the syncytial cables of the PMCs. (**A**) Whole-mount in situ hybridization using the *SpSlc4a10* antisense probe demonstrated high expression levels of this gene in the cell bodies of PMCs and staining is also found in the syncytial cables. (**B**) High-magnification image of four PMCs and the filopodia of the PMC syncytium that are positively stained.
DOI: https://doi.org/10.7554/eLife.36600.004

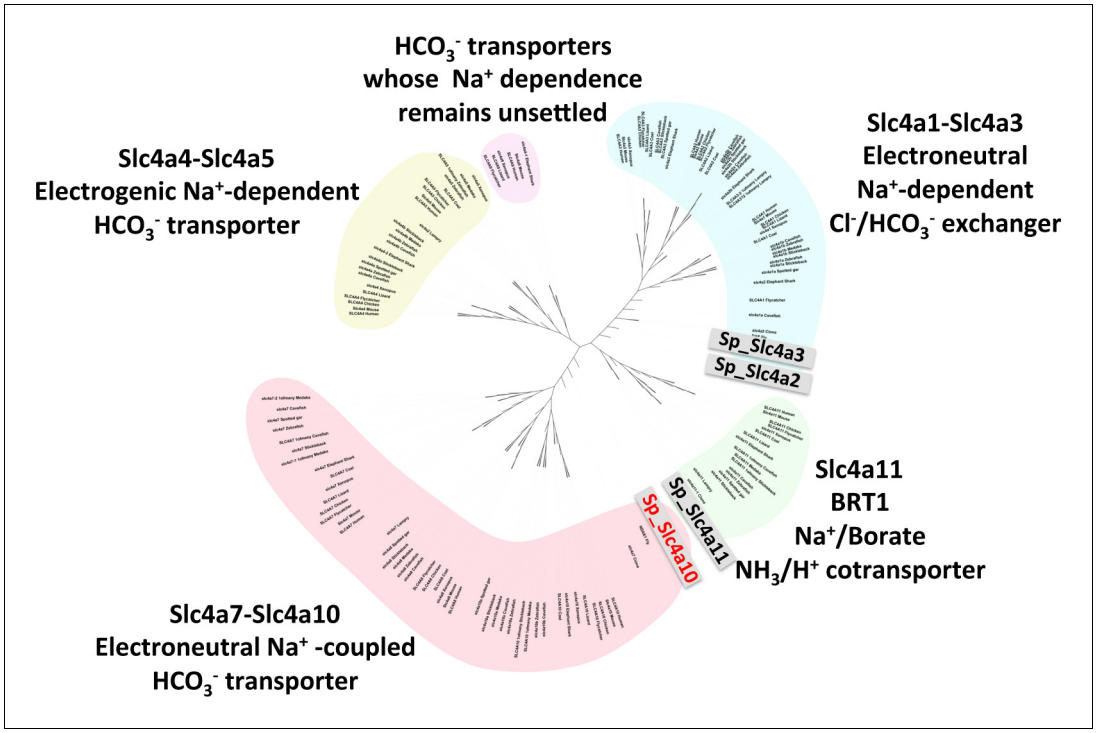

Figure 1—figure supplement 2. Phylogeny of vertebrate and sea urchin Slc4 transporters. Phylogenetic analysis performed on deduced amino acid sequences of the four *S. purpuratus* SLC4 family transporters and those from vertebrates and other marine invertebrates (see ***Supplementary file 1***-Table S1 for sequence information).
DOI: https://doi.org/10.7554/eLife.36600.005

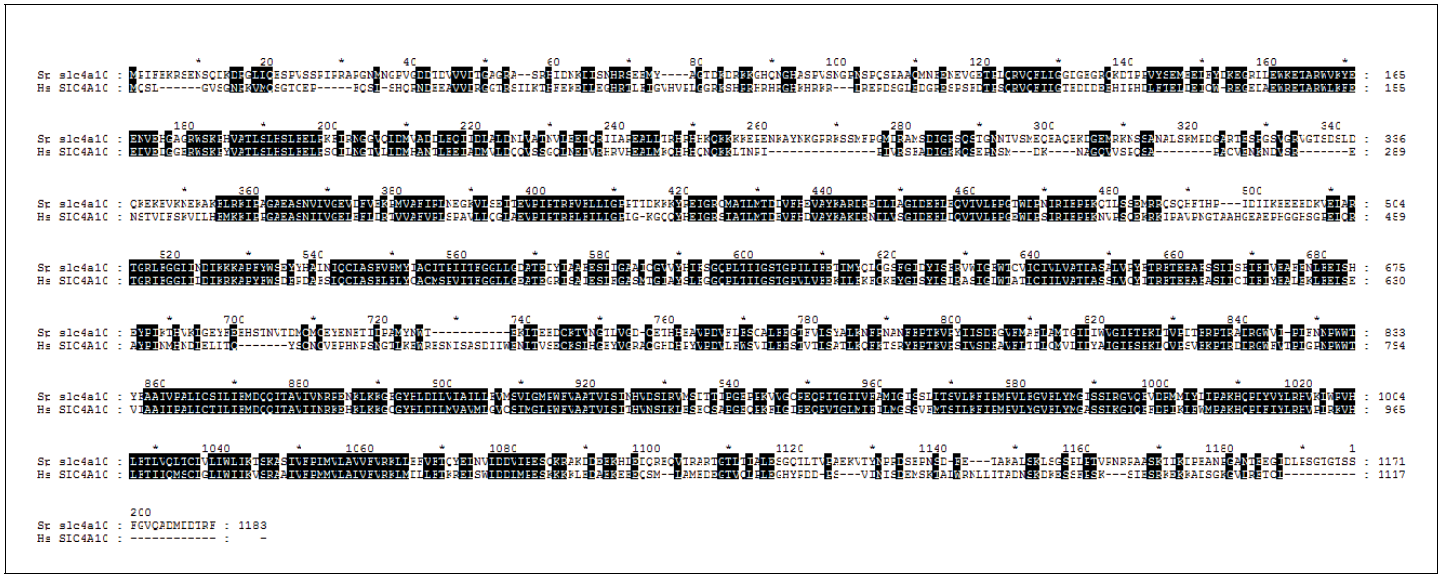

Figure 1—figure supplement 3. Sequence alignment of the human NBCn2 (Slc4a10) and the sea urchin SpSlc4a10. Alignment of deduced amino acid sequences demonstrates 44% identity between the human Slc4a10 and the sea urchin SpSlc4a10.

DOI: https://doi.org/10.7554/eLife.36600.006

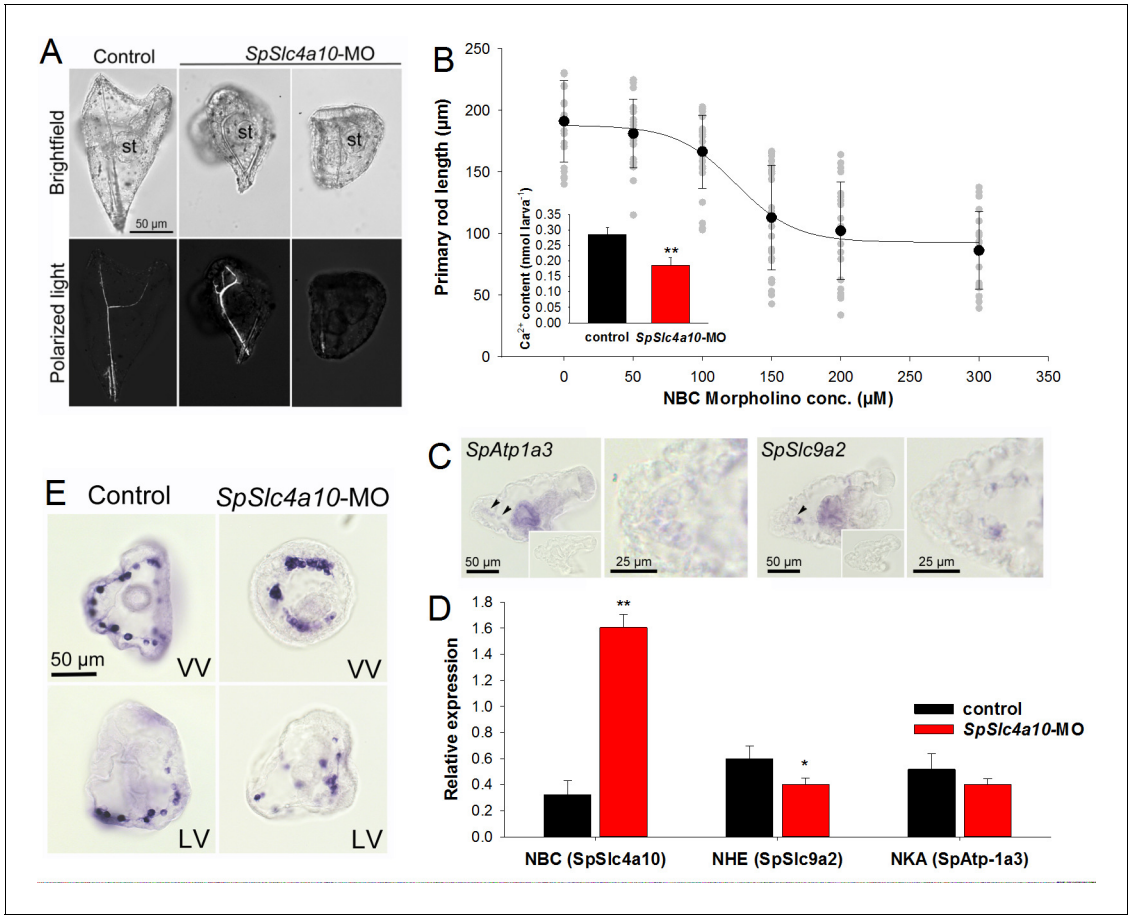

Figure 2. Morphological and molecular characterization of the *SpSlc4a10* morphant. (**A**) Light microscopic analyses with polarized light (birefringence) were used to detect deformations of the larval skeleton in *SpSlc4a10* morphants (4 dpf). The tri-partite digestive tract is normally developed in the *SpSlc4a10* morphants (st, stomach). (**B**) Length of the primary rod and total calcium content (inset) were used as indicators for reductions in calcification in 4 dpf morphants. Grey dots indicate individual measurements from experimental replicates (n = 4) (**C**) Expression of *SpAtp1a3* (Na^+/K^+-Atpase; NKA) and *SpSlc9a2* (Na^+/H^+-exchanger; NHE) in PMCs and stomach epithelial cells. (**D**) mRNA levels of *SpSlc4a10, SpAtp1a3 and SpSlc9a2* in control and *SpSlc4a10*-MO injected larvae. (**E**) Ring formation (2 dpf) of the *SpSlc4a10* expressing PMCs is disrupted in *SpSLC4a10* morphants (LV, lateral view; VV, vegetal view). Bars represent mean ± SD; *n* = 3–4 (*p<0.05; **p<0.01).

DOI: https://doi.org/10.7554/eLife.36600.007

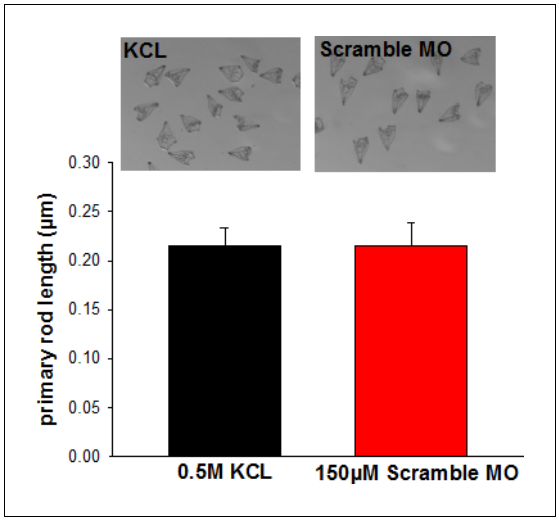

Figure 2—figure supplement 1. Comparison of KCL and scramble morpholino (MO) injected larvae. The primary rod length was used as an indicator for skeletal deformations. Fertilized eggs were injected with 0.5 M KCL, the vehicle of the MOs used in the present work. The concentration of the scramble morpholino was adjusted to 150 µM which corresponds to the concentration of SpSlc4a10 MO used for all experiments.

DOI: https://doi.org/10.7554/eLife.36600.008

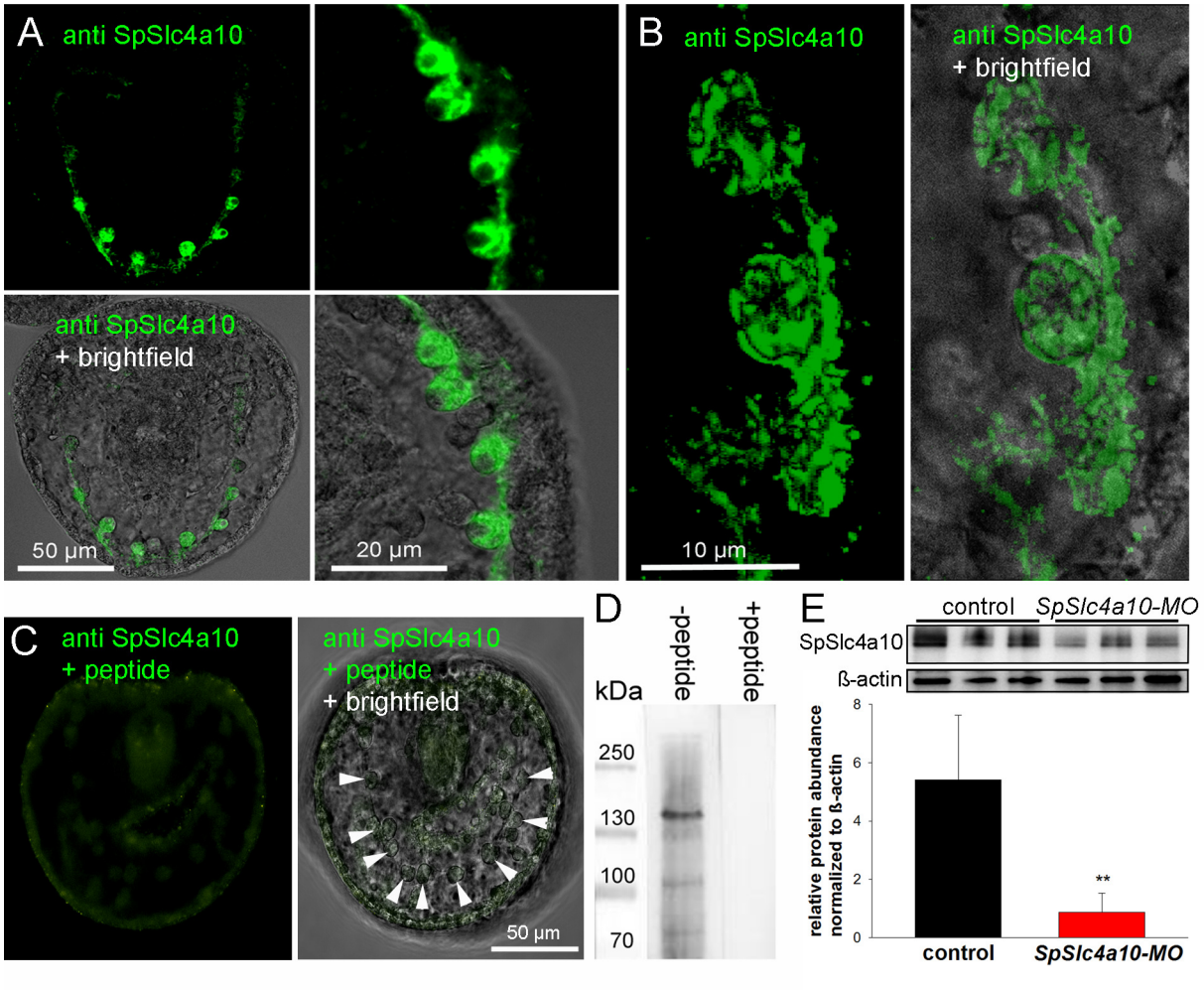

Figure 3. Localization of the SpSlc4a10 protein in PMCs and validation of the morpholino knock-down. (**A**) Immunohistological analyses using a custom made antibody designed against the sea urchin SpSlc4a10 protein demonstrating high concentrations of this protein in PMCs of late gastrula larvae (2 dpf). (**B**) High-magnification confocal microscopy showing the sub-callular localization of the SpSlc4a10 protein. (**C**) Negative controls were performed by blocking the primary antibody with the immunizing peptide (PMCs indicated by arrowheads) (**D**) Westernblot analysis demonstrated specific immunoreactivity of the SpSlc4a10 antibody with a 135 KDa protein that disappeared in the peptide compensation assay. (**E**) Validation of the SpSlc4a10 knock-down by quantification of protein levels using western-blot analyses. Bars represent mean ±SD; $n = 3$ (**p<0.01).

DOI: https://doi.org/10.7554/eLife.36600.009

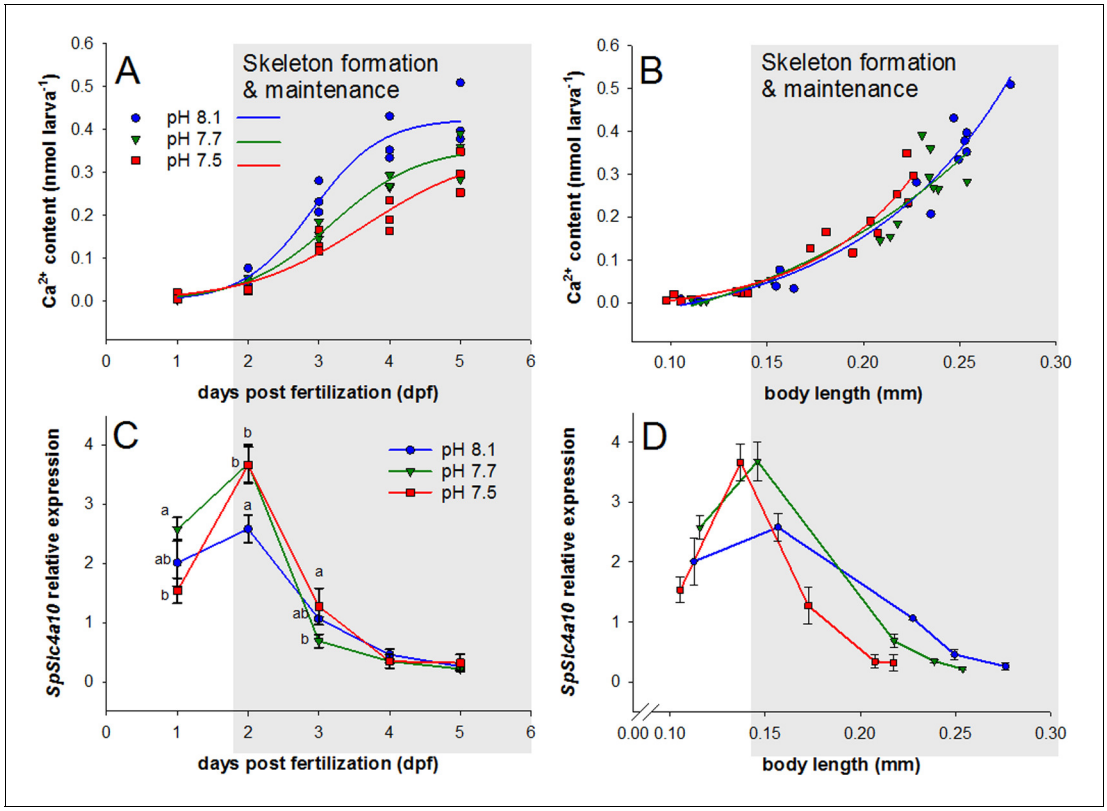

Figure 4. Development, calcium accumulation and expression of *SpSlc4a10* in sea urchin larvae raised under experimental ocean acidification. (**A**) Total Ca^{2+} content of larvae raised under three different pH conditions. (**B**) Larval Ca^{2+} content plotted as a function of body length to normalize for the developmental delay caused by acidified conditions (for morphometric analyses see Supplemental information ***Figure 4—figure supplement 1***). (**C**) *SpSlc4a10* mRNA levels normalized to the housekeeping gene *SpZ12* during development under different pH conditions. (**D**) Expression pattterns for *SpSlc4a10* along the early development plotted as a function of body length. Different letters denote significant differences between treatments. Bars represent mean ± SD; $n = 3$.

DOI: https://doi.org/10.7554/eLife.36600.010

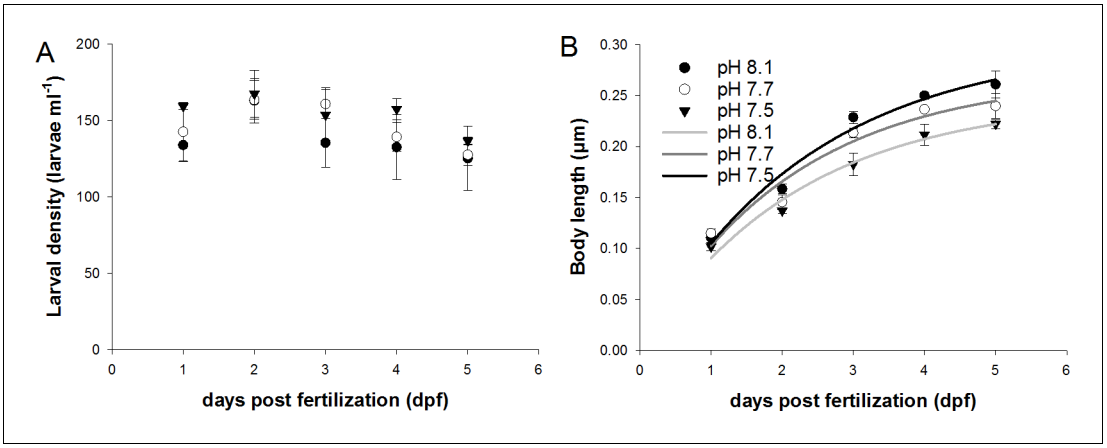

Figure 4—figure supplement 1. Mortality and growth of sea urchin larvae raised under different pH treatments. (**A**) Larval densities were constant at 140 to 160 larvae per ml over the experimental duration of 5 days. No effects on the larval densities were observed between the three pH treatments. Larval growth expressed as body length (BL) followed a logarithmic curve along the period of 5 days. Regression analyses demonstrated significant differences in BL between the three pH treatments. Values are presented as mean ± SD.

DOI: https://doi.org/10.7554/eLife.36600.011

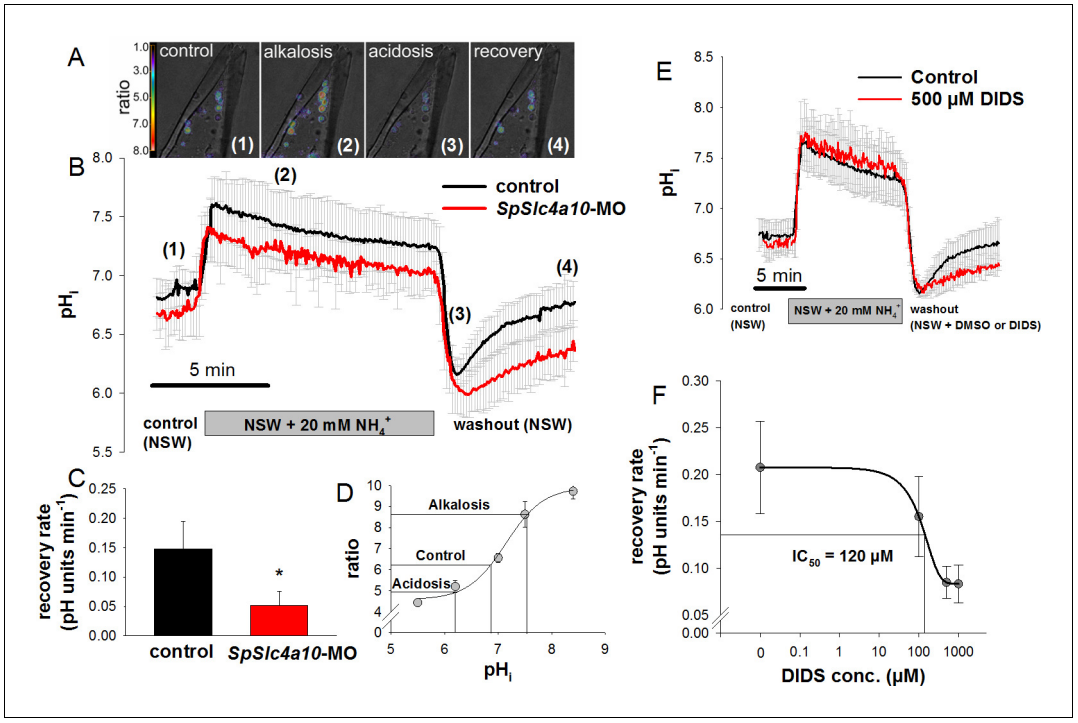

Figure 5. Intracellular pH regulatory abilities of primary mesenchyme cells. (**A**) Ratiometric fluorimetry in primary mesencyme cells (PMCs) using the pH sensitive dye BCECF-AM. False colour images superimposed on transmission images at time points 1, 2, 3, 4 as indicated in (**B**). (**B**) Summarized data from the control period (control (1)), after addition and removal of NH_3/NH_4^+ (alkalosis (2) and acidification (3); ammonium pulse), and during pH_i recovery (4). (**C**) The recovery rate of the *SpSlc4a10* morphants was significantly reduced (see ***Supplementary file 1***-table S2 for summary of prameters measured). (**D**) Calibration curve of BCECF-AM in PMCs obtained at different pH levels in the presence of the ionophore nigericin and 150 mM K^+ allowing the translation of ratios to pH values. (**E**) Acid–base regulatory abilities of PMCs in the presence of 500 µM DIDS or only the vehicle (DMSO) as control. (**F**) The recovery rate from an intracellular acidosis is inhibited by DIDS in a dose-dependent manner with an IC_{50} value of 120 µM. Bars represent mean ±SD; *p<0.05 (*n* = 4–5 larvae with 3–5 cells measured per larvae).

DOI: https://doi.org/10.7554/eLife.36600.012

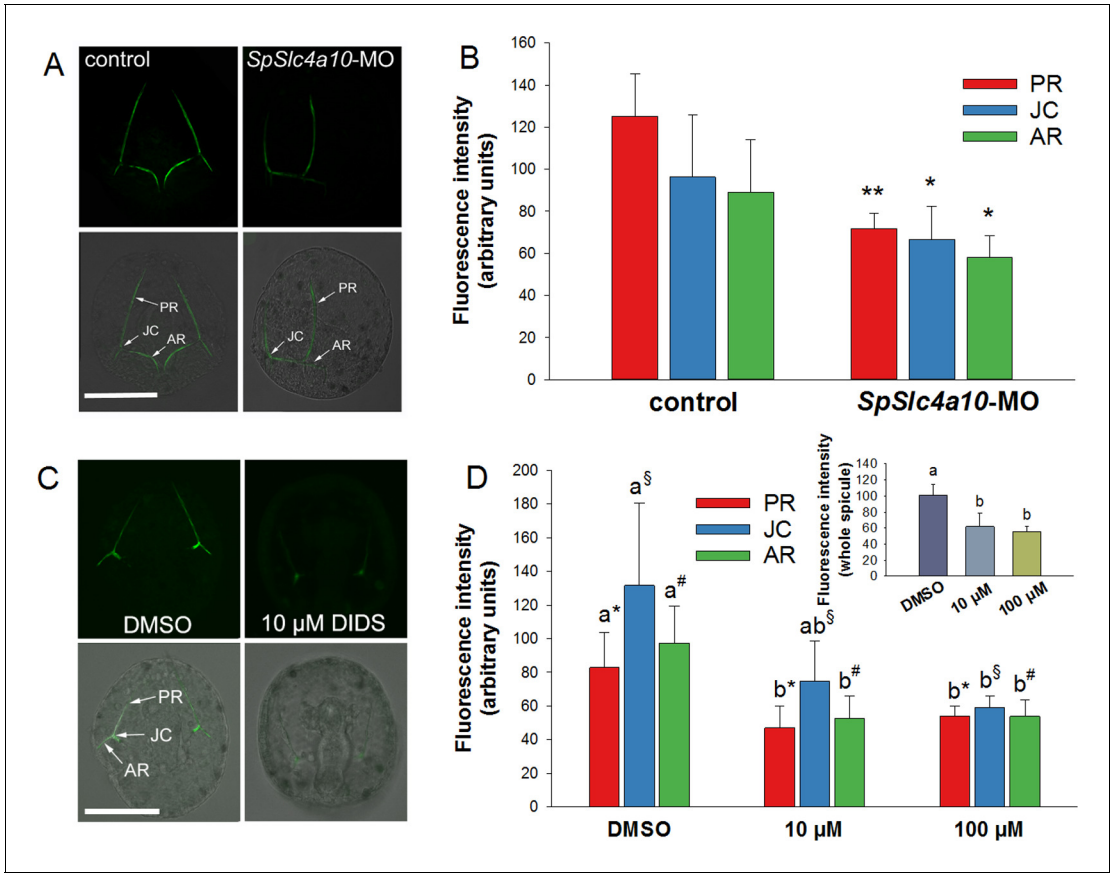

Figure 6. Calcein pulse–chase experiments to determine Ca^{2+}incorporation into spicules during inhibition and knock-down of HCO_3^- transport pathways. (**A**) Larvae of the late gastrula stage (2 dpf) were incubated in 160 µM calcein for 3 hr and confocal microscopy was used to determine fluorescence intensities in the spicules at different locations (posterior rod: PR, junction: JC, anterior rod: AR) after the calcein pulse. (**B**) Flourescence intensities are decreased in the morphants in all three locations. (**C**) Calcein incorporation in the presence of 10 µM DIDS or only the vehicle (DMSO) as control. (**D**) Fluorescence intensities, reflecting the amount of Ca^{2+} precipitated into spicules during the calcein pulse, decreased in DIDS-treated larvae in a dose-dependent manner (inset: intensities for entire larval skeleton). Values are presented as mean ± SD; *n* = 4 (with 2–3 larvae per replicate experiment: 9–11 individuals). Different letters denote significant diffrences between treatments. Same symbols used in ***Figure 5D*** indicate groups that were compared by one-way ANOVA. *p<0.05; **p<0.01.

DOI: https://doi.org/10.7554/eLife.36600.013

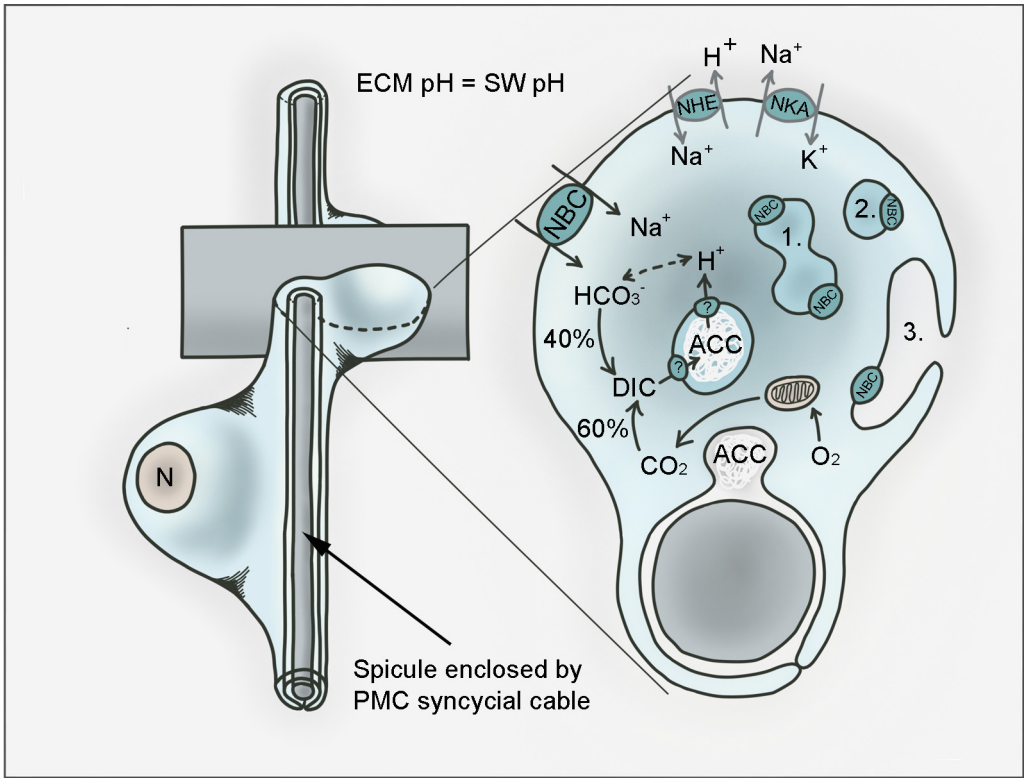

Figure 7. Hypothetical model for pH regulation and bicarbonate transport in PMCs of the sea urchin larva. PMCs form a syncytium within the extraxellular matrix (ECM) that has a pH the same as sea water (SW) in which the larva develops. Amorphous calcium carbonate (ACC) is precipitated in intracellular vesicles and exocytosed to the growing calcite spicule. Dissolved inorganic carbon (DIC) is provided through endogenous (i.e. respiratory CO_2) as well as exogenous (from the sea water) sources. *SpSlc4a10* (NBC) is proposed to mediate the import of bicarbonate from the seawater and to buffer protons generated during the precipitation of $CaCO_3$. Protons are exported from the vesicles through so far unknown pathways. Protons accumulating in the cytoplasm are potentially exported by the Na^+/H^+-exchanger (NHE) *SpSlc9a2*. Both secondary active transporters, NBC and NHE are driven by the Na^+/K^+-ATPase (NKA; *SpAtp1a3*) that is highly expressed by PMCs. In addition to its localization in the plasma membrane, NBC is associated with intracellular compartments including vesicles (1), vesicular networks (2) and vesicles fusing with the plasma membrane (3). n; nucleus.

DOI: https://doi.org/10.7554/eLife.36600.014